JOURNAL OF COMPUTATIONAL PHYSICS 1, 496-516 (1967)

A Nonlinear Computer Model Applicable to Low-Beta Plasma Interchange Modes in Two Dimensions[1]

J. A. BYERS

Electronics Research Laboratory, Department of Electrical Engineering, University of California, Berkeley, California 94720

ABSTRACT

A two-dimensional, two-fluid, nonlinear computer model that is applicable to low-beta plasma interchange modes is described. Two, oppositely charged, interpenetrating fluids are followed in their two-dimensional motions perpendicular to a strong magnetic field with guiding center drift velocities by a finite-difference integration of the equations of continuity. The model is very similar to models in incompressible hydrodynamics. Primary among these similarities are the procedures and problems of spatial finite-differencing; these aspects are discussed only briefly. The new features brought in by the plasma characteristics have caused problems in computational stability of the method of time finite-differencing; the analysis and solution of these problems are discussed extensively. In particular, the frequently used leapfrog scheme is found to be unconditionally unstable due to growing computational modes and other schemes, along with model changes to a "one-fluid" model in certain regimes, are found to be necessary for stability. Of more general interest to other nonlinear fluid models that deal with the integration of equations of the form $\partial u/\partial t = F(u, t)$ is the derivation of composite schemes that retain some of the desirable qualities of several single schemes.

I. INTRODUCTION

Plasma instabilities at large amplitudes are obtained by computer calculation of the two-dimensional motion of an ion fluid and an electron fluid. The two charge fluids move with guiding center velocities in applied magnetic and gravitational fields, with self-electric field due to net charge or charge separation. The calculation is basically *Eulerian*, with densities, velocities and potentials, etc., known only at the two-dimensional grid points. There are similarities with incompressible ($\nabla \cdot \mathbf{v} = 0$) hydrodynamic flows. This approach is in contrast with nearly all

[1] The research reported herein was supported in part by the Electronic Technology Division, Air Force Avionics Laboratory Research and Technology Division, Wright-Patterson Air Force Base, Ohio, under Contract No. AF33(615)-1078/3524 and by the Joint Services Electronics Program (U. S. Army, U. S. Navy and U. S. Air Force) under Grant No. AF-AFOSR-139-66.

previous plasma computer experiments that have followed the motion of super particles such as sheets or disks or rods and are essentially Lagrangian.

The two fluids are tenuous, coexist in the same space, and subject to similar forces. The relatively light electrons are not allowed to undergo the forces that are proportional to mass; hence, there is a difference in fluid velocities. The difference causes charge separation, hence an electric field **E**. This field in turn acts with the magnetic field, **B**, to produce oscillatory or exponentially growing motion starting from small perturbations. The growth to large amplitude can lead to expansion of the plasma from its initial shape, to a new but locally *confined* state or to pumping of plasma to a wall, a *nonconfined* state. One objective of the program is to determine the final state of (known) instabilities when the plasma is excited initially at small amplitudes.

The plasma is neutral or nearly so and is immersed in a magnetic field **B** and external force field **g**. The velocities of the two fluids are obtained from guiding-center theory [1]. Each fluid obeys an Eulerian equation of continuity; the equations are used to advance the densities at each time step. The net charge density, $e(n_1 - n_e)$, is used in Poisson's equation to obtain the potential, ϕ. The new electric field changes the velocities, the fluid divergence, and hence, the densities. Then the cycle restarts.

Plasma interchange is considered as meaning cooperative, charged particle motion, perpendicular to the magnetic field, **B**. The ratio of the plasma pressure to the magnetic field pressure is so low that changes in the value of **B** due to the plasma currents can be ignored. The strong magnetic field is also justification for the two-dimensionality. The effects of B field curvature are simulated by a gravitational field, $\mathbf{g}(\perp \mathbf{B})$. The guiding-center-drift description of a plasma is known to be valid for many low-frequency phenomena (e.g., see [2]). The effects of finite size of gyro orbits can be included in the drift description as correction factors [3]. The physical theory and initial results are reported elsewhere [4].

Here we present the computer-experiment design with emphasis on two distinct computational problems arising out of the time-finite-differencing procedures:

(1) Specific procedures of time finite-differencing of equations of the form $\partial u/\partial t = F(u, t)$. (This should be of interest to the general reader.)

(2) A computational stability problem arising from the computational formulation of a particular plasma characteristic.

II. Model, Fields, Variables, General Program, and Governing Equations

The model is shown in Fig. 1. There are two applied fields: magnetic field **B**, and general force (or gravitational) field **g**, $\mathbf{g} \perp \mathbf{B}$. Both are uniform in space and

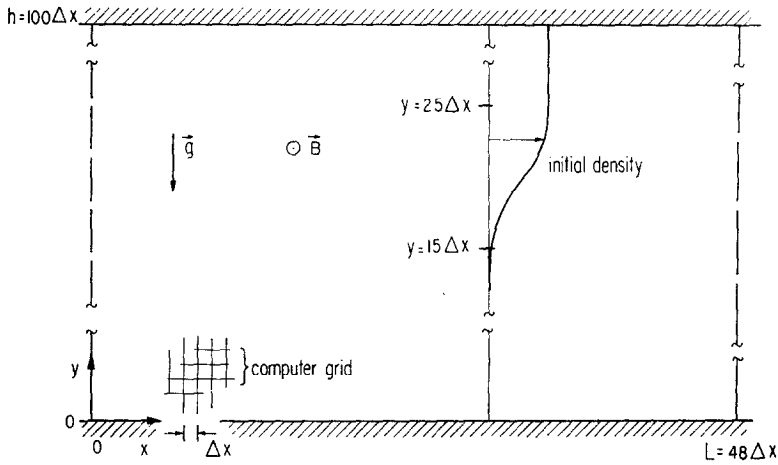

FIG. 1. Model description. Plasma is between conducting walls at $y = 0$, $100\,\Delta x$ in uniform **g** and **B** fields. Initially, the plasma is uniform except for a boundary layer that extends about 10 grid cells. L is the Fourier period, the maximum wavelength observable. The boundary-layer development can be followed only in the lower half of the grid, $y \leqslant 50\,\Delta x$, due to computer storage limitations.

constant in time. The region is bounded at $y = 0$, $y = h$ by conducting walls at zero potential, $\phi = 0$; in x, the model is assumed to be periodic with period $L = 48\Delta x$.

The independent variables are x, y, and t. The dependent variables are: the electron and ion charge densities, n_e , n_i; the potential (due solely to net charge or charge separation, $n_i - n_e$); the corresponding electric field $E = -\nabla\phi$; and the electron and ion fluid guiding-center velocities, $\mathbf{v}_e$ and $\mathbf{v}_i$. The following are the governing equations:

$$\nabla^2\phi = -e(n_i - n_e)/\epsilon_0\,, \tag{A}$$

$$E = -\nabla\phi, \tag{B}$$

$$\mathbf{v}_e = \mathbf{E} \times \mathbf{B}/B^2, \tag{C}$$

$$\mathbf{v}_i = \mathbf{E} \times \mathbf{B}/B^2 + m/e \cdot \mathbf{g} \times \mathbf{B}/B^2 + m/eB^2 \cdot d\mathbf{E}/dt, \tag{D}$$

$$\partial n_i/\partial t = -\nabla \cdot (n_i\mathbf{v}_i), \tag{E}$$

$$\partial n_e/\partial t = -\nabla \cdot (n_e\mathbf{v}_e). \tag{F}$$

In differential form with continuous variables, these would be solved simultaneously. In difference form the solutions will be obtained at the points $x = i\,\Delta x$, $i = 1, 2, \ldots, 48$, $y = j\,\Delta y$, $j = 1, 2, \ldots, 48$, and at times $t = 0$, Δt, $2\Delta t$, etc.

The general program proceeds as follows: Initially, densities n_i and n_e are given.

From these, the potential ϕ, electric field $\mathbf{E}$, and hence guiding-center velocities are found, all at one time level. The calculations involving the differencing of $\partial/\partial t$ require storage at more than one time level. The new values of the densities n_i and n_e at the new time level are obtained from difference solutions of the equations of continuity, Eqs. (E) and (F).

We are describing a plasma where the cooperative motion of both charge species is a slow $\mathbf{E} \times \mathbf{B}/B^2$ drift of guiding centers across the externally imposed magnetic field. This guiding-center drift description of charged-particle motion demands only that all frequencies are small compared to the ion gyro frequency,

$$\omega \ll \omega_{ci},$$

and that all macroscopic lengths be much larger than the ion gyro radius,

$$L \gg a_i.$$

These requirements impose a restriction on the maximum allowable net charge density:

$$|n_i - n_e| m_i/(\epsilon_0 B^2) \ll 1.$$

Note that $K = n_i m_i/(\epsilon_0 B^2)$ can still be much larger than unity if $|n_i - n_e|$ is sufficiently small. K is a critical parameter and is a measure of the effectiveness of the plasma to changes in the electric field.

The assumption that the magnetic field B is constant in time requires that all plasma currents be sufficiently low. This essentially is the "low-beta" approximation and is a restriction on the magnitude of "thermal" velocities or simply that the plasma thermal energy density be much less than the magnetic energy density.

Readers familiar with existing, incompressible, hydrodynamic models will recognize the close relationship with this plasma model. In one limit where we follow only a single charge species with $\mathbf{v}_E = \mathbf{E} \times \mathbf{B}/B^2$, this plasma model is exactly analogous to those hydro-dynamic models where the charge density plays the role of the vorticity (the component perpendicular to the plane of motion), and the electrostatic potential plays the role of the stream function. The new feature in this plasma model is then the presence of two oppositely charged fluids where the net charge density is obtained from the difference between the densities of those fluids. The significance of this is that when the two charge fluids have approximately equal densities, even small relative velocities are important because they can cause separation and, hence, lead to changes in the electric field. This is the reason that the last two terms in the ion velocity are important (similar terms are ignored for the electrons because of the large mass ratio). The $m_i/eB^2 \cdot \mathbf{g} \times \mathbf{B}$ term leads to charge separation and is the reason for the existence of flutes

(Rayleigh–Taylor modes) in the plasma. (Rosenbluth and Longmire, [5] 1957, for a guiding center drift derivation of the flute instability.) The last term, $m_i/eB^2 \cdot d\dot{\mathbf{E}}/dt$. known as the polarization drift, also leads to charge separation and is the reason for the existence of the low-frequency plasma dielectric constant, $\epsilon_0(1 + K)$, where

$$K = n_i m_i/(\epsilon_0 B^2).$$

It is this polarization drift which leads to strong computational instability when using the "usual" procedure for time differencing (the leapfrog or midpoint scheme). Later sections deal with alternative time differencing methods that retain some of the desirable qualities of the leapfrog scheme, and with the analysis and resolution of the computational instability due to the polarization drift.

III. Spatial Grid, Storage Requirements, and Time Levels

The grid used has 48×48 cells. The upper wall is placed at $y = 100\Delta x$ so it has only a small effect on the potential in the region of the boundary layer that is initially centered at $y = 20\Delta x$. Motion for $y \geqslant 48\Delta x$ cannot be followed.

As a minimum, n_i, n_e, and ϕ are stored at past and present time levels. This requires $3 \times 2 \times 48 \times 48 = 13,824$ locations. Since the program is long, this amount is close to the practical limit of the IBM 7094 without external storage.

IV. Spatial Finite-Differencing Procedures

The spatial differencing procedures used on this model are well-known, ordinary space-centered, fluid-conserving schemes.

The method used for solving the five-point finite-difference form of Poisson's equation is like that of Hockney [6] which is a fast, direct solution that proceeds, by Fourier analysis of the charge density along each row, solving for the potential Fourier amplitudes, and finally synthesizing the actual potentials at each grid point by summing the Fourier terms along each row. The method appears to be considerably faster than any known relaxation method. Knowledge of the Fourier mode amplitudes for the charge density and electrostatic potential can also be a useful diagnostic.

During the integration of the equation of continuity, fluid conservation is obtained by using a space-centered difference analog of $\nabla \cdot (nv)$ which, in the simplest 2-point form in one dimension, is

$$[(nv)_{j+1} - (nv)_{j-1}]/(2\Delta x). \tag{1}$$

With the interpretation of $n_j = \int_{-\Delta x/2}^{+\Delta x/2} n\,dx = N_j$, the total fluid in the cell of dimension Δx centered about the grid point j, it is clear that the flux in the total fluid for cells $j + 2$ and $j - 2$ will include contributions that exactly cancel the flux in total fluid for cell j, as given by Eq. (1). This scheme has the somewhat unpleasant aspect that adjacent cells are uncoupled. (Even-numbered cells cancel the fluid flux in other even-numbered cells, and odd-numbered cells cancel the fluid flux in other odd-numbered cells.) In one particular model, it is known that this property is the cause of a nonlinear computational instability at short wavelengths [7]. Lilly [8] shows that this particular instability can be avoided by using certain spatial-differencing schemes. Many other spatial-differencing schemes of the same order of accuracy are possible and, indeed, are used in many nonlinear fluid calculations.

The property of exact fluid conservation may not be very important. The formulation of a difference scheme in a particular manner so as to conserve a given quantity exactly may, in fact, be detrimental in that the conservation property will be satisfied even if significant computational errors occur. The conservation property therefore loses its value as an independent check of the accuracy of the calculation.

It is known that nonlinear fluid calculations frequently encounter serious computational stability problems (evidenced by large amounts of spurious energy appearing in short wavelengths) due to the spatially differenced terms. In many models, artificial damping is included to control short wavelengths.

The nonlinear processes effectively generate spatial harmonics of the dependent variables so that the k spectrum grows wider. For $k > k_{\max} = \pi/\Delta x (\lambda < 2\Delta x)$, the differencing interprets the k as a smaller value, *aliasing*, as $k_{\text{new}} = k - k_{\max}$ (e.g., $\lambda = 4/3\Delta x \rightarrow \lambda_{\text{new}} = 4\Delta x$). Lilly [8] shows, in a special case, that aliasing errors are comparable to those of the finite-difference Laplacian. Aliasing, however, can also produce a nonlinear computational instability due to consistent error buildup at small λ over long times; one particular problem of this type is the Phillips [7] instability mentioned above.

Our code at present has no methods guarding against severe consistent truncation error appearing in short wavelengths. Short-run calculations, as are appropriate for some simple single "events," may not be plagued by such problems. That is, the complete calculation may be of sufficiently short duration that errors in short wavelenghts do not have enough time to build up to dangerous levels. Several successful short-run calculations [4] were made with the present model with little or no evidence of short-wavelength problems. Other calculations with the present model, applied to more complicated situations with a requirement for somewhat longer computer runs, presented computational stability problems of exactly this nature. Completely successful runs will require some form of control on short wavelengths.

The finite orbit corrections to the guiding-center drift equations can be expressed entirely with a simple addition to the ion equation of continuity. This additional term involves the spatial operators, ∇ and ∇^2. These spatially differenced terms complicate the short-wavelength problem mentioned above, but nothing fundamentally new is added to the spatial-differencing problem.

V. Time Differencing Procedures; Use of Composite Schemes

The main problem in this effort was numerical instability of finite difference equations which are analogs of the equation

$$\partial u/\partial t = F(u, t), \tag{2}$$

which is the general form of the continuity equations [Eqs. (E) and (F) above]. Truncation error, one problem, is measured by comparing Eq. (2) with a Taylor-series expansion of the finite-difference form of Eq. (2); the net error that results from the *cumulative* addition of a single time-step truncation error must remain small. Practically all nonlinear fluid calculations are restricted by computer storage limitations to time difference schemes that use information at two time levels to predict the new values. There are still a large number of schemes in this class however, and they differ widely in their accuracy and stability properties. The "best" choice of scheme usually depends on the particular type of solution expected.

Here we examine the stability (cumulative truncation error) of several schemes used to solve the oscillator equation

$$\partial u/\partial t = i\omega u. \tag{3}$$

Lilly [8] and Kurihara [9] present comparative lists of several schemes as applied to Eq. (3). In this section we construct and analyze *composite* schemes that retain some of the desirable properties of several schemes. The analytic solution of Eq. (3) is of course

$$u(t) = u_0 \exp(i\omega t).$$

The finite difference solution of Eq. (3) should correspond as closely as possible to the constant amplitude oscillation of the analytic solution. We have obtained composite difference schemes that maintain a nearly constant amplitude and tolerable errors in phase.

A second problem is to eliminate or damp the extraneous computational modes that always occur when the difference scheme is of higher order than the continuous differential equation. Under certain conditions, our equations are subject to a

particularly strong computational instability due to growing computational modes. This problem is discussed in Section VI. The damping of computational modes is a requirement on any composite scheme we derive.

Before describing the derivation of composite schemes we first describe five single difference schemes, all well known, which yield fairly good approximate solutions of Eq. (3). All five schemes however are deficient in one of the two desirable qualities, constancy of the amplitude of the physical mode, or damping of computational modes. These five single schemes are then used in various combinations for successive time steps in an attempt to obtain a net *composite* scheme which comes closer to satisfying both criteria.

The leapfrog (Lf) scheme applied to the general equation, Eq. (2), is, with time levels indicated by superscripts,

$$(u^1 - u^{-1})/(2\Delta t) = F^0,$$

where the truncation error is $\sim\partial^3 u/\partial t^3$. To obtain the solution of a finite-difference equation, we follow the conventional technique described by Richtmyer [10] who represents the difference solution of $u(n\Delta t)$ as

$$u^n = \lambda^n u^0,$$

where the λ's are called the amplification factors. Thus, for Lf applied to Eq. (3), where we have

$$u^1 - u^{-1} = 2ibu^0 \qquad \text{with} \quad b = \omega\Delta t,$$

the characteristic equation is

$$\lambda - 1/\lambda = 2ib,$$

or

$$\lambda = ib \pm (1 - b^2)^{1/2},$$

and λ_+ corresponds to the physical mode and λ_- corresponds to an extraneous computational mode. Note that $|\lambda_\pm| = 1$ if $b^2 \leqslant 1$. The physical mode therefore shows no error in the amplitude of the wave. The computational mode in this case does not grow or damp. Unfortunately, Lf is subject to a strong computational instability when applied to our equations (see Section VI), and must be rejected.

The Adams–Bashforth (AB) scheme as applied to Eq. (2) is

$$(u^1 - u^0)/\Delta t = \tfrac{3}{2} \cdot F^0 - \tfrac{1}{2} \cdot F^{-1},$$

where the truncation error is again $\sim\partial^3 u/\partial t^3$. For AB applied to Eq. (3) we have

$$u^1 - u^0 = \tfrac{3}{2}ibu^0 - \tfrac{1}{2}ibu^{-1},$$

which results in the characteristic equation

$$\lambda^2 - \lambda(1 + \tfrac{3}{2}ib) + \tfrac{1}{2}ib = 0.$$

When $b \ll 1$, this yields

$$|\lambda_+| = 1 + 0b^4 + \cdots,$$

i.e., a small amplification of the physical mode, and

$$|\lambda_-| = \tfrac{1}{2}b \ll 1,$$

i.e., a large damping of the computational mode. The amplification of the physical mode may not be tolerable for long time observation.

A third scheme, which is an iterative procedure, is Heun (H). Applied to Eq. (2), it is

$$u^* - u^0 = \Delta t F^0, \tag{4}$$

$$u^1 - u^0 = \tfrac{1}{2}\Delta t (F^0 + F^*). \tag{5}$$

Here, u^* and F^* refer to tentative first guesses for the new values. Applying H to Eq. (3), we obtain a small amplification of the physical mode,

$$|\lambda| = 1 + 0b^4.$$

There are no computational modes.

The fourth and fifth schemes, Lfc and ABc, are similar, corrector iterative procedures where tentative u^* is obtained by Lf or AB, then corrected by averaging F as in Eq. (5). Both Lfc and ABc damp computational modes, and both yield a small damping of the physical mode,

$$|\lambda_+| = 1 - 0b^4 + \cdots.$$

The damping may not be tolerable for long time observation.

Composite schemes, which use various combinations of the five schemes given above for successive time steps, have been tested with respect to Eq. (3). The object was to obtain *partial cancellation* of truncation errors and damping of computational modes. The net effect is more subtle, however, than simply adding errors of opposite "sign." For example, as applied to Eq. (3), Lf (no growth) + AB (slow growth) gives net slow damping.

Kurihara [9] tested the Lfc scheme as applied to Eq. (3), and suggested that the Lfc damping might be minimized by using it only intermittently with Lf. Our results show that this is not necessarily so; indeed, the composite scheme Lf–Lfc gives small amplification.

When dealing with composite schemes it is more convenient to use a matrix formulation which for Lf applied to Eq. (3) is

$$\begin{bmatrix} u^1 \\ u^0 \end{bmatrix} = \begin{bmatrix} 2ib & 1 \\ 1 & 0 \end{bmatrix} \begin{bmatrix} u^0 \\ u^{-1} \end{bmatrix}.$$

The characteristic equation for the eigenvalue λ is then obtained in the usual way, i.e., $\mathrm{Det}|\, \mathsf{A} - \lambda \mathsf{I}\, | = 0$, where A is the amplification matrix. This formalism makes it immediately obvious why the net effect of a composite scheme is not simply the product of the eigenvalues of the individual parts. To each eigenvalue there corresponds an eigenvector, in two-level schemes such as Lf, composed of a fraction of u^0 and a fraction of u^{-1}. Another two-level scheme, such as AB, will have a different eigenvector and thus the net eigenvalue or amplification factor of the composite scheme cannot be simply the product $\lambda_{\mathrm{Lf}} \cdot \lambda_{\mathrm{AB}}$. The amplification matrix for the composite scheme is simply the product of the individual matrices. Thus, for AB. Lf we have

$$\begin{bmatrix} u^1 \\ u^0 \end{bmatrix} = [\mathrm{Lf}] \begin{bmatrix} u^0 \\ u^{-1} \end{bmatrix} \qquad \text{and} \qquad \begin{bmatrix} u^2 \\ u^1 \end{bmatrix} = [\mathrm{AB}] \begin{bmatrix} u^1 \\ u^0 \end{bmatrix}$$

which gives

$$\begin{bmatrix} u^2 \\ u^1 \end{bmatrix} = [\mathrm{AB}][\mathrm{Lf}] \begin{bmatrix} u^0 \\ u^{-1} \end{bmatrix}.$$

The evaluation of the composite eigenvalue now proceeds as usual. Schemes of varying levels can also be used; e.g., to use Lf alternating with a three-level scheme we merely change the description of Lf to

$$\begin{bmatrix} u^1 \\ u^0 \\ u^{-1} \end{bmatrix} = \begin{bmatrix} 2ib & 1 & 0 \\ 1 & 0 & 0 \\ 0 & 1 & 0 \end{bmatrix} \begin{bmatrix} u^0 \\ u^{-1} \\ u^{-2} \end{bmatrix}.$$

Using this technique we have analyzed 20 different composite schemes composed of various combinations of the five single schemes described previously. Most of these composite schemes exhibit amplitude errors of the same order of magnitude as the five single schemes. (The single-scheme Lf has no amplitude errors, but as noted previously, it must be rejected because of computational mode growth.) Four of these 20 composite schemes show a great reduction in amplitude errors and retain a strong damping of computational modes. Table I is a summary of the $|$ amplitude $|^2$ after about eight cycles for five single and 20 composite schemes. Figure 2 shows the amplitudes for the four best schemes given in the table as a function of $b = \omega\, \Delta t$. Phase errors are not shown; they were comparable for all schemes and were tolerably small.

TABLE I

A LIST OF VARIOUS COMPOSITE SCHEMES COMPARED WITH RESPECT TO THE SOLUTION OF THE EQUATION $\partial u/\partial t = i\omega u$ [a]

Scheme No.	Description of scheme	Number of single schemes used	$\lvert R \rvert^2$ at $\omega T = 50$ for $\omega\Delta t =$ 0.1	0.2	0.3
1	Lf	1	1.000	1.000	1.000
2	AB	1	1.025	1.24	2.25
3	H	1	1.012	1.12	1.45
4	Lfc	1	0.975	0.83	0.57
5	ABc	1	0.975	0.82	0.54
6	Lf–AB	2	0.977	0.85	0.65
7	Lf–Lfc	2	1.026	1.24	2.11
8	AB–ABc	2	1.012	1.09	1.30
9	Lf–ABc	2	1.025	1.20	1.73
10	AB–H	2	1.025	1.23	2.03
11	Lf–Lf–AB	3	1.025	1.21	1.68
12	Lf–Lf–Lf–AB	4	0.979	0.90	0.86
13	Lf–Lf–Lf–Lf–AB	5	1.023	1.12	1.02
14	Lf–Lf–Lf–Lf–Lf–AB	6	0.982	0.95	1.12
15	Lf–AB–AB–AB	4	1.006	1.05	1.20
16	Lf–Lf–AB–AB–AB	5	1.025	1.22	1.97
17	Lf–AB–AB–AB–AB	5	1.010	1.09	1.36
18	Lf–Lf–AB–AB–AB–AB	6	1.025	1.23	1.50
19	Lf–Lf–AB–AB	4	1.025	1.22	1.91
20	Lf–AB–Lf–AB–AB	5	0.990	0.93	0.82
21	Lf–AB–AB–H–Lf	5	1.025	1.20	1.73
22	Lf–H	2	1.0002	1.008	1.063
23	Lf–AB–AB	3	0.9996	0.990	0.946
24	Lf–AB–AB–Lf–H	5	0.997	0.984	0.978
25	AB–Lf–AB–Lf–H	5	1.00004	1.002	1.021

[a] Any individual scheme yields an amplification $u^n/u^0 = Re^{i\theta}$, whereas the analytic solution amplification is $u(n\Delta t)/u^0 = 1.0 \exp(in\omega\Delta t)$: $\lvert R \rvert^2$ at $\omega T = 50$ (≈ 8 cycles) is given for several values of $\omega\Delta t$. $T = n\Delta t$.

Table I should not by any means be considered an exhaustive list of composite schemes. Indeed even the choice of the single schemes is arbitrary, although we have found these to be the most useful. The technique described in this section can be used to analyze a composite scheme composed of any combination of single schemes.

The method of comparison used in Table I may be unfamiliar to readers

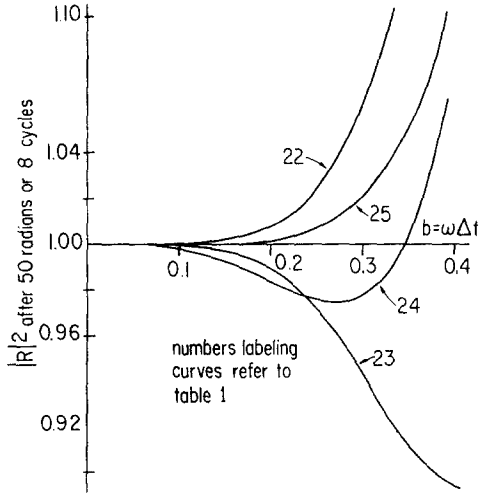

FIG. 2. Square of amplitude vs $\omega \Delta t$ at $\omega T = 50$ for the four best schemes of Table I.

accustomed to seeing the single step amplification factor written out as an expansion in $b = \omega \Delta t$. Thus, the AB scheme yields $|\lambda|^2 = 1 + 0.54b^4 + \cdots$ and the H scheme yields $|\lambda|^2 = 1 + \frac{1}{4}b^4$. (Lilly [8] reports that the AB scheme yields $|\lambda|^2 = 1 + \frac{1}{4}b^4 + \cdots$, which is slightly in error.) These single-step expressions cannot be directly compared with the expansions for the multistep composite schemes; thus, a fixed comparison time ($\omega T = 50$) was chosen for Table I. A rough comparison of the above expressions with the expansions for one of the better composite schemes, however, does reveal the dramatic improvement obtainable; thus, Lf–H, scheme No. 22 of Table I, yields (for the two time-step amplification factor) $|\lambda|^2 = 1 + b^6$.

There may appear to be undue emphasis on the simple equation, Eq. (3), as our numerical procedure does not actually involve integration of this equation. But since we expect many oscillating or wave-type solutions, the above analysis and our problem should agree, at least qualitatively. Several schemes from Table I (Nos. 1, 2, 4–6, 13, 23, 24) have been tried in our program when the linear analysis predicts a simple oscillating solution. Numbers 1 and 13 were unstable due to growing computational modes, as will be discussed in the next section. The other schemes were stable to computational modes, and in all cases the predictions of Table I were confirmed. That is, with $\omega \Delta t = 0.3$, there was good quantitative agreement between the predictions of Table I and the actual results obtained. (Most of these schemes were tested before their analysis was attempted; the relatively large damping and amplification led to the analysis.)

Various composite schemes with combination Lf–H worked well in linear regimes but in certain nonlinear calculations produced a growing $2\,\Delta t$ oscillation, i.e., a time splitting that is characteristic of computational instability. The time-splitting sensitivity of Lf is well known. Here, the time splitting appears to be a reaction of Lf against the greater error which occurs in H in nonlinear regimes when v is function of n. The present program uses scheme No. 23 almost always.

VI. Time-Differencing Instability Due to Computational Modes

A. *General Discussion*

It is well known that Lf is computationally unstable when used with the equation

$$\partial u/\partial t = -\omega u.$$

The characteristic equation for the Lf scheme is

$$\lambda^2 + 2b\lambda - 1 = 0, \qquad \text{where} \quad b = \omega\,\Delta t.$$

This yields

$$\lambda_{\pm} = -b \pm (1 + b^2)^{1/2}.$$

Note that $|\lambda_-| < 1$; therefore, the computational mode grows and quickly dominates the solution. Contrast this with AB scheme where the characteristic equation is

$$\lambda^2 - \lambda(1 - \tfrac{3}{2}b) - \tfrac{1}{2}b = 0,$$

or

$$\lambda_{\pm} = \tfrac{1}{2}(1 - \tfrac{3}{2}b) \pm \tfrac{1}{2}(1 - b + \tfrac{9}{4}b^2)^{1/2},$$

and note that $|\lambda_-| \ll 1$ for small b. This means that the AB scheme will cause a large damping of the computational mode.

Our equations are subject to a dangerous instability due to growing computational modes when the Lf scheme or an Lf-dominated composite scheme such as No. 14 of Table I is used. A complete stability analysis of the entire problem using the technique described by Richtmyer [10] is easily formulated but is not easily solved. The best that can be done in most complicated system is to isolate each part and to determine the subsystem stability conditions. The hope is, of course, that the sum of such separate stability conditions will also be sufficient for stability for the actual system. This is the procedure we followed. (It is worth pointing out, however, that Kasahara [11] found an example where just this subsystem procedure was found to fail.)

B. *Time Differencing of Continuity Equation*

The term that produces instability in the plasma problem is the polarization drift in the ion velocity. Accordingly, we ignore other terms and examine the subsystem that is a reasonable approximation of the actual system.

Writing the charge densities as

$$\rho_1 = en_1, \qquad \rho_e = -en_e, \qquad \rho = \rho_1 + \rho_e = e(n_1 - n_e), \tag{6}$$

we obtain from Eqs. (E), and (F), an equation for the net charge density,

$$\partial\rho/\partial t = -e\nabla \cdot (n_i\mathbf{v}_i - n_e\mathbf{v}_e). \tag{7}$$

For illustration, net flux will be taken as due to velocity difference which allows us to use

$$n_1 \approx n_e = n.$$

$v_1 - v_e$ comes from $v_g(\sim m\mathbf{g} \times \mathbf{B})$ and $v_p(\sim m\, d\mathbf{E}/dt)$. Since the troublesome part is $\partial E/\partial t$ in dE/dt, we will use $v_p \sim m\, \partial E/\partial t$ and ignore v_g. (The common drift $v_E \gg v_p$.) Thus, approximately,

$$\partial\rho/\partial t = -\nabla \cdot (nm_1/B^2 \cdot \partial\mathbf{E}/\partial t) + \cdots. \tag{8}$$

Replacing ρ with $-\epsilon_0\nabla^2\phi$ and $\mathbf{E} = -\nabla\phi$, and expanding the divergence, we obtain an equation in n and ϕ,

$$\partial(\nabla^2\phi)/\partial t = -nm/\epsilon_0 B^2 \cdot \partial(\nabla^2\phi)/\partial t - m/\epsilon_0 B^2 \cdot [\partial(\nabla\phi)/\partial t] \cdot \nabla n + \cdots. \tag{9}$$

In solving, we estimate the right-hand side (r.h.s.) from past and present times and the value obtained is used to predict new values; the details depend on the differencing scheme used, as will be shown. The two $\partial(\nabla^2\phi)/\partial t$ terms are *not* combined; as in our *two-fluid* model this equation is not solved explicitly.

For simplicity, let n be taken as a zero-order variable and let the variations of ϕ be along only one coordinate, $x = j\Delta x$. Let $\nabla\phi$ be given by the two-point expression $(\phi_{j+1} - \phi_{j-1})/(2\Delta x)$ and $\nabla^2\phi$ by the three-point expression

$$(\phi_{j+1} - 2\phi_j + \phi_{j-1})/\Delta x^2.$$

Let ϕ be given by a Fourier expansion,

$$\phi(x) = \phi(j\Delta x) = \sum_k \phi^k \exp(ikj\,\Delta x). \tag{10}$$

Thus, Eq. (9) is, for a given k,

$$\partial\phi^k/\partial t = nm/\epsilon_0 B^2 \left\{-1 + \frac{i\nabla n}{kn} \cdot \frac{\sin k\Delta x}{k\Delta x}\left[\frac{k\Delta x/2}{\sin(k\Delta x/2)}\right]^2\right\} \frac{\partial\phi^k}{\partial t} + \cdots \tag{11}$$

$$= [-K + iKD]\, \partial\phi^k/\partial t + \cdots. \tag{12}$$

The r.h.s. may use present and past times; the l.h.s. may use past, present, and future times.

Lf differencing gives (dropping the Fourier index k)

$$\phi^1 - \phi^{-1} = (-2K + 2iKD)(\phi^0 - \phi^{-1}),$$

which uses past and present times on the r.h.s. and past and future on the l.h.s. Using

$$S = -2K + 2iKD,$$

we find that the characteristic equation is

$$\lambda^2 - S\lambda - (1 - S) = 0.$$

The physical mode solution is

$$\lambda_+ = 1,$$

and the computational mode solution is

$$\lambda_- = -1 + S$$

with

$$|\lambda_-|^2 = 1 + 4K + 4K^2 + 4K^2D^2 > 1.$$

The inequality holds as $K = n_1 m_1/\epsilon_0 B^2 > 0$. Hence this mode is unconditionally unstable.

AB differencing gives

$$\phi^1 - \phi^0 = \tfrac{1}{2}S[\tfrac{3}{2}(\phi^0 - \phi^{-1}) - \tfrac{1}{2}(\phi^{-1} - \phi^{-2})]$$

with the characteristic equation

$$\lambda^3 - \lambda^2(1 + \tfrac{3}{4}S) + \lambda S - \tfrac{1}{4}S = 0.$$

The physical mode is

$$\lambda = 1,$$

and there are two computational modes obtained from

$$\lambda^2 - \tfrac{3}{4}\lambda S + \tfrac{1}{4}S = 0.$$

For negligible D, marginal stability, $|\lambda| = 1$, holds for one of these modes for $K = 0.5$; for the other $|\lambda| = 0.25$, hence is damped.

Composite schemes from Table I, not dominated by Lf, are stable for $K \lesssim 1$. In general, schemes which are composed of a larger fraction of Lf are harder to stabilize, i.e., the larger the percentage of Lf, the lower the marginal stability value of K. Lf dominated schemes, like No. 14, are unstable unless $K \ll 1$.

There should be some mention about the possible magnitudes of the coefficient

$$D = \frac{\nabla n}{kn} \cdot \frac{\sin k\Delta x}{k\Delta x} \cdot \left[\frac{k\Delta x/2}{\sin(k\Delta x/2)}\right]^2.$$

The trigonometric function varies from 1.0 to 0.0 as $k\,\Delta x$ increases from 0 to π or $\lambda = 2\Delta x$, as short as can be "seen" on the spatial grid. The $\nabla n/kn$ term is roughly $1/k\delta$ where δ is the thickness of the boundary layer. The difficulty arises here at *small k, long wavelength.* If taken at face value, it means that even the AB scheme would be unstable due to some long-wavelength effect of the polarization drift on the electrostatic field. The source of the trouble is the difference analog of the Laplacian operator ∇^2. Similar problems with this term have appeared in previous stability analyses (Charney *et al.* [12]), where it was remarked that long-wavelength instability not predictable on the assumption that $D \lesssim 1$.

The computational mode behavior of those schemes of Table I that we have tried (Nos. 1, 2, 4–6, 13, 23, 24) agrees very well with the foregoing analysis. There is evidence that the long-range nature of the electrostatic field allows the stability condition to be violated in part of the region if it is satisfied sufficiently strong elsewhere. Thus in scheme No. 6, the stability analysis yields $nm/\epsilon_0 B^2 = \frac{1}{3}$ as the condition of marginal stability, but the numerical solution with $n_{\max} m/\epsilon_0 B^2 = 0.5$ was perfectly stable (n varies from 0 up to $n_{\max}$). In many systems this behavior does not occur, i.e., stability conditions must be satisfied everywhere [10].

Unless $K \ll 1$, there is an additional damping of the physical mode caused by the inaccuracy of our finite-difference form for $\partial\phi/\partial t$ at $t = 0$; $(\phi^0 - \phi^{-1})/\Delta t$ has an error term $\sim\partial^2\phi/\partial t^2$. The damping of course is reduced as $\omega\,\Delta t$ is reduced but is quite large at $\omega\,\Delta t = 0.3$ if $K \sim 1$. A more accurate finite difference expression is

$$(\tfrac{3}{2}\phi^0 - 2\phi^{-1} + \tfrac{1}{2}\phi^{-2})/\Delta t,$$

but this requires storing another array of numbers corresponding to ϕ^{-2} and may not be feasible because the storage requirements are already quite high. The use of more time steps also introduces more computational modes which may result in more stringent stability conditions. For example, with the use of this more accurate expression for $\partial\phi/\partial t$, the Lf scheme is more strongly unstable, and the AB scheme allows a K only one half as large as previously for marginal stability.

Thus, by restricting K to $\lesssim 1$, various difference schemes that are stable to the polarization term can be devised. This is not an entirely satisfactory situation however, because it would be desirable to have K range over values from $\ll 1$ to $\gg 1$. In the next section, the changes in the model necessary for $K \gtrsim 1$ are described.

VII. Round-Off Errors; One-Fluid Model

In the last section we showed that the source of the computational mode difficulty in our two-fluid model is the ion polarization velocity, $\mathbf{v}_p = m_i/(B^2e) \cdot d\mathbf{E}/dt$, which represents the response of the plasma to changes in $\mathbf{E}$. The higher the value of $K = n_i m_i/(\epsilon_0 B^2)$, the more effective the plasma is in responding to changes in $\mathbf{E}$. As K is increased to large values, the resulting net charge separation becomes very small, $|n_i - n_e| \ll n_i$. Even if the two-fluid model were computationally stable, there would be increased round-off errors as $K \gg 1$, due to taking the difference of nearly equal values.

To surmount both the round-off error and the computational instability inherent in the two-fluid model, we change the program from two-fluid to *one-fluid.* Instead of following the electron fluid and ion fluid separately, we follow a neutral fluid ($n = n_i \approx n_e$) and a charged fluid ($n_c = n_i - n_e$) with E/B drifts only; the remaining ion drifts, v_g, v_p, are used only to cause charge separation. (These approximations imply that $v_E \gg v_g$ which usually is a good assumption when $K \gtrsim 1$.)

The change in the computational stability criterion can be easily calculated. Eq. (8) (corrected for the terms omitted in the previous discussion) in the one-fluid model is now solved explicitly so we can combine $\nabla^2\phi$ terms changing Eq. (9) to

$$\partial(\nabla^2\phi)/\partial t = \frac{-m/\epsilon_0 B^2 \cdot \partial(\nabla\phi)/\partial t \cdot \nabla n}{(1 + nm/\epsilon_0 B^2)} + \cdots. \tag{13}$$

Eq. (12) becomes

$$\frac{\partial\phi}{\partial t} = i\frac{K}{1+K} D \cdot \frac{\partial\phi}{\partial t} = iD' \cdot \frac{\partial\phi}{\partial t} + \cdots. \tag{14}$$

The stability condition for the AB scheme is now that D' be of the order $\lesssim \frac{1}{2}$ and is satisfied (if D itself is sufficiently small) whatever the value of K. This behavior is typical of most of the schemes of Table I. Lf is still unstable (although not as strongly), but the Lf-dominated schemes may not be. For example, No. 14 is marginally stable when $D' \approx 0.25$. All of the schemes of Table I were not tested with respect to the polarization term in the one-fluid model, since most of the schemes had already been rejected on the criterion of the damping or amplification of the physical mode.

In the range $K \lesssim 1$, the one-fluid model can provide a check against the round-off error in the two-fluid model. Some runs have been made with both the one-fluid model and the two-fluid model, where the behavior was expected to be one-fluid in nature (E/B drift dominating). No essential differences were found, so we feel confident that, in some cases at least, round-off error in the two-fluid model is not serious.

VIII. Output: Energy vs Time, Fourier-Mode Amplitude vs Time, Marker-Particle Trajectories

As diagnostic computer output, the electric, kinetic, and gravitational energies are followed in time and the total energy, of course, is to be conserved. Energy plots are frequently a good early indicator of computational trouble.

The time behavior of spatial Fourier modes (we have periodicity in x) is available for more detailed understanding and for developing nonlinear theory. The Fourier amplitudes for $\rho = e(n_i - n_e)$ and $\phi[\rho^k(y)$ and $\phi^k(y)]$ are obtained each time step as part of the potential solution. Hence, no additional computation is required.

The primary initial objective has been to obtain growth to large amplitude of

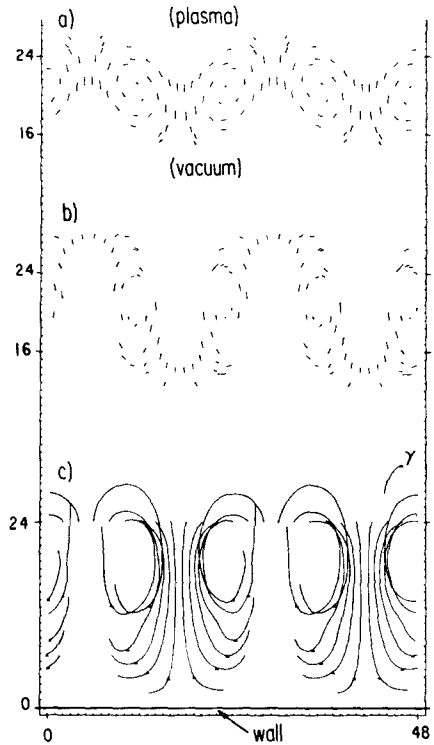

FIG. 3. Rayleigh–Taylor instability growth. Marker-particle positions and velocity vectors are shown at two intermediate times: (a) $t = 7.200$; (b) $t = 9.350$; (c) shows the trajectories for the entire run, ending at $t = 12.975$ for those particles initially on line $y = 24\ \Delta x$. The small triangles mark the positions at $t = 11.775$. $t = 7.200$ corresponds to approximately 5e-folding times of the linear theory. γ is the last part of a trajectory for a particle initially on the bottom row at $(x, y) = (48\ \Delta x, 16\ \Delta x)$. Boundary initially extends from $y \approx 15\ \Delta x$ ($n = 0$ for $y < 15\ \Delta x$) to $y \approx 25\ \Delta x$ ($n = n_{max}$ for $y > 25\ \Delta x$).

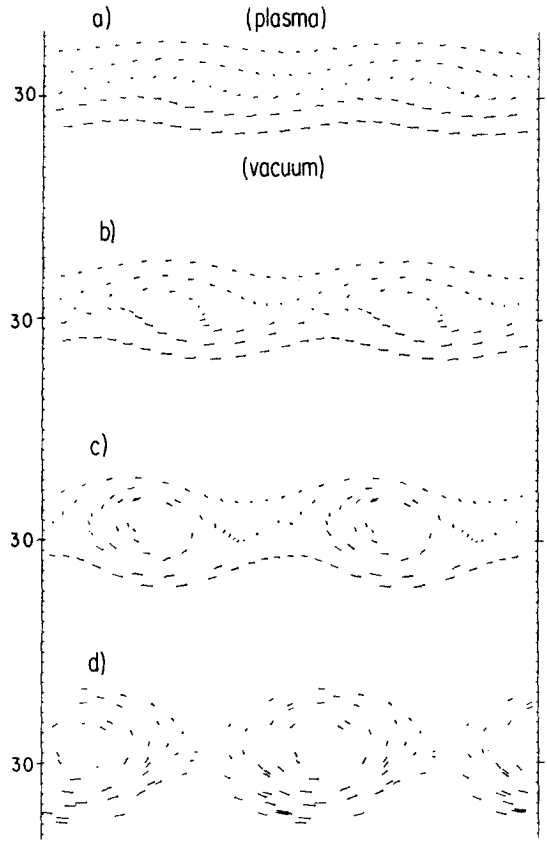

FIG. 4. Kelvin–Helmholtz instability growth. Marker-particle positions and velocity vectors are shown at four different times: (a) 15 Δt; (b) 30 Δt; (c) 60 Δt; (d) 120 Δt. The center of the boundary layer is at $y = 30$ as marked. Conducting wall is at $y = 0$. $\Delta t \approx 0.5\, \Delta x / V_{\max}$.

various boundary-layer instabilities. It was especially desirable to distinguish instabilities that saturated, with plasma spatially *confined*, from those that pumped plasma to the wall or were *nonconfined*. Initial results showed that the Rayleigh–Taylor growth was nonconfined but that the Kelvin–Helmholtz growth was confined—both for low densities, $K \ll 1$ (see [4]). The development was followed with plots of *marker particles*, which are points with forward pointing "tails" giving velocity vectors. Snapshots and time exposures or trajectory plots were obtained. The marker particles are fictitious particles inserted (usually uniformly) in the plasma and followed with local E/B velocity. Examples are given in Figs. 3 and 4.

IX. Conclusions

The nonlinear plasma model described in this report has many characteristics of older models in incompressible hydrodynamics. The main new feature of this plasma model is that the motion of two interpenetrating fluids is calculated. These two fluids, which are oppositely charged, move with guiding center drifts perpendicular to a strong magnetic field **B**, and are driven by two different velocity fields, which, however, are nearly identical; the $\mathbf{v}_E = \mathbf{E} \times \mathbf{B}/B^2$ is velocity is common to both fluids. In the velocity of the ion fluid there are small additional terms that lead to net charge separation and, hence, to a change in the electric field **E**, which is the driving term. These additional terms in the ion velocity are also the source of severe computational instability of the method of time differencing. One frequently used method of time differencing, the leapfrog (Lf) scheme, is unconditionally unstable due to growing computational modes. Other schemes, such as the Adams–Bashforth (AB) and Heun (H) schemes are stable provided certain restrictions are imposed on the allowable magnitude of an important physical parameter, $K = n_1 m_1/\epsilon_0 B^2$, which is a measure of the response of the plasma to changes in the electric field. No stable time finite-difference scheme is possible in the two-fluid model for $K \gtrsim 1$. When $K \gtrsim 1$, physical conditions (related to the problem of round-off), as well as the stability conditions, dictate a change to a "one-fluid" model, where a neutral fluid and a charged fluid are followed with v_E drifts only, and a net charge separation is calculated from the small additional ion drifts. Analysis and actual tests of the model show that stability for $K \gtrsim 1$ is indeed possible in the one-fluid model. Rejection of the leapfrog scheme for the time integration also led us to search for composite schemes (where alternate time steps use different single schemes) which retain some of the desirable qualities of several individual schemes. Several composite schemes, which use the single schemes Lf, AB, and H in various combinations, have been devised which, while retaining much of the computational mode stability of AB and H, are also very close to the desirable property of the Lf scheme, the nonamplification of the amplitude of oscillating solutions. These last results should be applicable to other nonlinear fluid models for which wave-type solutions are expected from the integration of equations of the type $\partial u/\partial t = F(u, t)$.

Acknowledgments

[redacted]

Birdsall engaged in numerous discussions and arguments (some at 8000 miles!) and collaborated on much rewriting of the manuscript.

Short discussions with Dr. J. Killeen and Dr. C. E. Leith were helpful in clarifying certain computational problems.

Thanks are also due Professors A. W. Trivelpiece and W. B. Kunkel for their careful reading and checking of the manuscript.

Computer time was donated by the University of California Computer Center in Berkeley.

REFERENCES

1. T. G. NORTHROP, "The Adiabatic Motion of Charged Particles." Interscience, New York (1963).
2. S. CHANDRASEKHAR, "Plasma Physics." University of Chicago Press, Chicago (1960).
3. M. N. ROSENBLUTH and A. SIMON, *Phys. Fluids* **8**, 1300 (1965).
4. J. A. BYERS, *Phys. Fluids* **9**, 1038 (1966).
5. M. N. ROSENBLUTH and C. L. LONGMIRE, *Ann. Phys.* **1**, 120 (1957).
6. R. W. HOCKNEY, "A Fast Direct Solution of Poisson's Equation Using Fourier Analysis." Stanford Electronics Laboratories Technical Report No. 0255-1 (1964).
7. N. A. PHILLIPS, An example of nonlinear computational instability, *in* "The Atmosphere and Sea in Motion, pp. 501-504. Rockefeller Institute Press in association with Oxford University Press, New York (1959).
8. D. K. LILLY, *Monthly Weather Rev.* **93**, 11 (1965).
9. Y. KURIHARA, *Monthly Weather Rev.* **93**, 33 (1965).
10. R. D. RICHTMYER, "Difference Methods for Initial Value Problems." Interscience, New York (1957).
11. A. KASAHARA, *Monthly Weather Rev.* **93**, 27 (1965).
12. J. G. CHARNEY, R. FJORTOFT, and J. VON NEUMANN, *Tellus* **2**, 237 (1950).